



CHORUS

This is the accepted manuscript made available via CHORUS. The article has been published as:

Superconductor-Insulator Transition in Long MoGe Nanowires

Hyunjeong Kim, Shirin Jamali, and A. Rogachev

Phys. Rev. Lett. **109**, 027002 — Published 9 July 2012

DOI: [10.1103/PhysRevLett.109.027002](https://doi.org/10.1103/PhysRevLett.109.027002)

Superconductor–Insulator Transition in Long MoGe Nanowires

Hyunjeong Kim, Shirin Jamali, and A. Rogachev

Department of Physics and Astronomy, University of Utah, Salt Lake City, Utah 84112, USA

(Dated: June 13, 2012)

Properties of one-dimensional superconducting wires depend on physical processes with different characteristic lengths. To identify the process dominant in the critical regime we have studied transport properties of very narrow (9-20 nm) MoGe wires fabricated by advanced electron-beam lithography in wide range of lengths, 1-25 μm . We observed that the wires undergo a superconductor–insulator transition (SIT) that is controlled by cross sectional area of a wire and possibly also by the width-to-thickness ratio. Mean-field critical temperature decreases exponentially with the inverse of the wire cross section. We observed that qualitatively similar superconductor–insulator transition can be induced by external magnetic field. Our results are not consistent with any currently known theory of the SIT. Some long superconducting MoGe nanowires can be identified as localized superconductors, namely in these wires one-electron localization length is much smaller than the length of a wire.

PACS numbers: 74.48.Na, 74.25.Dw, 74.40.+k

One-dimensional systems play a special role in physics since they allow a more simple theoretical description than their counterparts in higher dimensions [1]. Moreover, experimental testing of 1D systems with finite length can probe the length scale of distinct physical processes. This possibility is important for systems that have long-range coherence in 3D, such as superconductors. In a one-dimensional limit superconductivity can be suppressed by several processes. In a microscopically disordered wire enhanced Coulomb repulsion competes with the Cooper pairing and suppresses an amplitude of order parameter [2]. In addition, a superconducting wire can acquire resistance due to phase slips, topological fluctuations of the order parameter. A phase slip can occur due to a thermally-activated fluctuation [4] or a quantum fluctuation (QPS) [3]. Recent theories suggest that the QPS rate can be suppressed both in wires shorter than the length of the phase propagation during a phase slip [5] and in very long wires due to attractive interaction between QPS with different signs [6]. The quantum state of a wire is also predicted to depend on the state [7] and impedance [8] of electrodes connected to a wire and on coupling to a dissipative environment [9–11].

Experimentally, there are at least two effects that cannot be explained by local physics. One is the anti-proximity effect in Zn [12] and Al [13] nanowires. The other is superconductor–insulator transition (SIT) in short MoGe nanowires [14, 15] (length 30-300 nm), which is controlled by the wire *normal state resistance* with separatrix set by $R_Q = 6.45 \text{ k}\Omega$. No QPS was detected in this work. Surprisingly, longer MoGe wires [16] did not reveal the SIT; instead a crossover was observed and interpreted in terms of the increasing rate of QPS. The QPS contribution and crossover behavior were also detected in long PbIn [17], Nb [18] and Al [19, 20] nanowires.

Experimental studies of 1D superconductors face a challenge of fabricating ultra-narrow *homogeneous* wires.

For amorphous MoGe alloys, this was achieved by deposition of MoGe on top of suspended carbon nanotubes. With this method, known as the molecular templating technique [21], wires with width down to 8 nm were fabricated and measured. Disadvantage of the method is that a wire can not be made sufficiently long; typically, the length is limited by 0.3 - 1 μm .

In the present work, we use an alternative fabrication method – high resolution electron beam lithography with negative resist [22, 23]. Details of fabrication are given in supplementary materials [24]. Figure 1A shows a scanning electron microscopy image of one of the nanowires used in transport measurements. Figure 1D schematically shows the cross section of a sample. The method does not have the length limitation. Another advantage is a possibility to make samples with a true 4-probe geometry as shown in Fig. 1C. In these samples, current electrodes, voltage probes and a wire are fabricated from the same original MoGe films. We fabricated and studied two series of nanowires from alloys with a distinct relative content of Mo and Ge: $\text{Mo}_{78}\text{Ge}_{22}$ and $\text{Mo}_{50}\text{Ge}_{50}$.

In Fig. 2A we plot resistance per unit length, $\rho_L(T) = R(T)/L$, for a series of $\text{Mo}_{78}\text{Ge}_{22}$ nanowires. The wires are labeled by letters and their length in micrometers is indicated in the parentheses. The other parameters of $\text{Mo}_{78}\text{Ge}_{22}$ nanowires are summarized in a table given in the supplementary materials [24]. The resistance of the wires increases by few percent when temperature decreases from 300 K down to 2-4 K. This behavior is typical for disordered systems; the gain is due to the weak localization and electron-electron interaction corrections [25]. The actual cross section area of nanowires, A , is not exactly known. The thickness of a wire is reduced from its nominal value (typically by 0.5-1 nm) due to oxidation and etching by the TMAH developer [24]. As shown in Fig. 1D, a MoGe nanowire is permanently covered by a 35-nm thick layer of exposed HSQ e-beam resist. However, the sides of a wire are not protected so the ac-

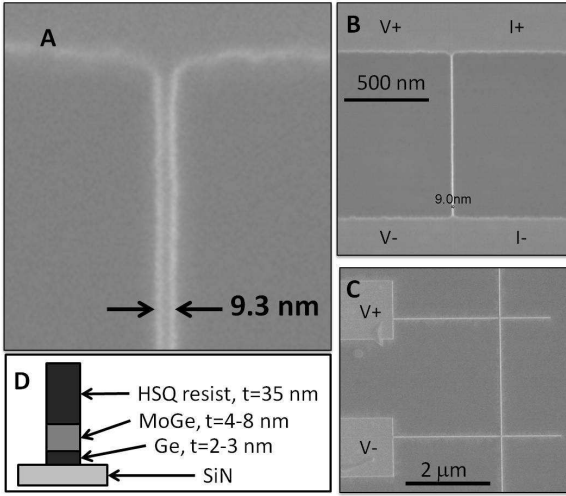


FIG. 1: (A) Scanning Electron Microscopy image of a nanowire. (B) Electrodes geometry for quasi-4-probe transport measurements used in majority of samples. (C) Electrodes geometry for 4-probe measurements with voltage-probe electrodes made of nanowires. Current electrodes are outside of the image. (D) Sketch of the cross section of a typical sample.

tual width of a wire can be reduced due to oxidation. Fortunately, MoGe films are known to have constant volume resistivity ($\rho = 160 \mu\Omega \text{ cm}$) down to thickness of 1 nm [28]. This property allows to estimate cross sectional area as $A = \rho L / R_{RT}$, where L is wire length and R_{RT} is resistance at $T=300 \text{ K}$.

All wires can be clearly separated in two groups: superconducting and insulating. Insulating wires (labeled as M,L,J) have resistance monotonously decreasing with temperature. As shown in Fig 2B, conductance in these wires can be well fitted by the dependence $G(T) = G_0 - \alpha/\sqrt{T}$ accounting for the electron-electron interaction in a normal disordered one-dimension metal (eq. 5.5 in Ref.[25]). The one-dimensional approximation is valid when the width of a wire is smaller than the thermal length $L_T = \sqrt{\hbar D / k_B T}$ [25]. With the diffusion coefficient of $\text{Mo}_{78}\text{Ge}_{22}$, $D = 0.5 \text{ cm}^2\text{s}^{-1}$ [26], this approximation is satisfied below 1.5 K. The presence of the SIT is also evident from nonlinear differential resistance shown in Fig 2C. The wires always show zero-bias anomaly that changes from negative to positive when the system crosses the SIT.

The lower panel of Fig. 2A shows $\rho_L(T)$ for superconducting wires. We observed that as the ρ_L in the normal state increases the superconducting transition shifts to low temperatures. Since for MoGe nanowires A is inversely proportional to $\rho_L(300\text{K})$ and in the normal state $\rho_L(T)$ depends on temperature weakly, we conclude that superconducting transition in MoGe nanowires is controlled by A . We notice that the sheet resistance is not

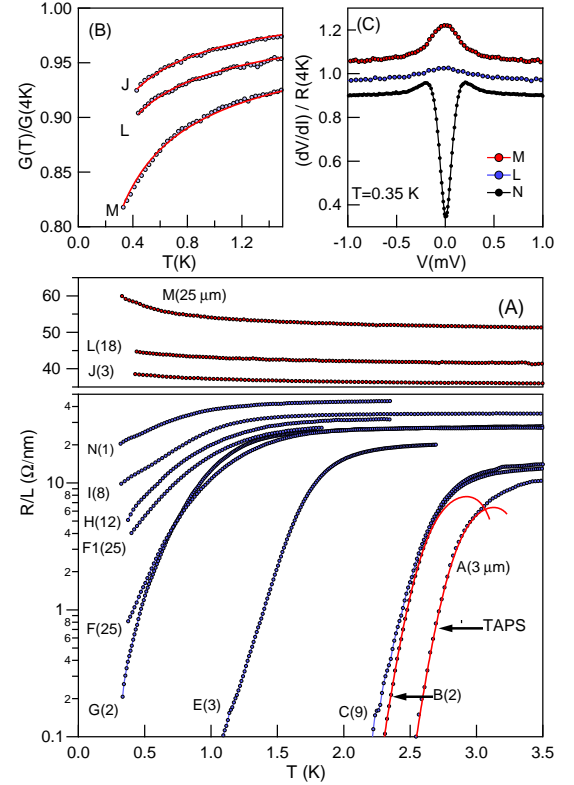


FIG. 2: (A) Resistance over length versus temperature for a series of $\text{Mo}_{78}\text{Ge}_{22}$ nanowires. Letters label the nanowires and numbers in the parentheses indicate the nanowire lengths in micrometers. For wires A and B, solid red lines are the fitting curves to the theory of thermally activated phase slips. (B) Normalized conductance as a function of temperature for insulating wires. Solid red lines are the fitting curves to the theory of electron-electron interactions in 1D. Data for wires L and M are downshifted by 0.02 and 0.04, respectively. (C) Normalized differential resistance at $T=0.35 \text{ K}$ for indicated wires. Data for wires L and N are downshifted by 0.05 and 0.1, respectively.

a critical parameter of the SIT. For example *insulating* wire J has sheet resistance $R_{\square} \approx 500 \Omega$, which in 2D limit corresponds to a *superconducting* film with $T_c \approx 3 \text{ K}$. We found that the cross sectional area of insulating wires J and L (53 and 44 nm^2 , respectively) is larger than that of superconducting wire N (37 nm^2). Wire N is the narrowest wire we have measured. It is possible that this wire has a granular structure due to non-uniform side oxidation. However, we also notice that wire J has nominal cross section $4 \times 17 \text{ nm}^2$ and wire N $6 \times 9 \text{ nm}^2$. So an alternative explanation is that for wires with the same A , the superconductivity is stronger when width-to-thickness ratio is closer to one. Possibly the effect occurs because electron-electron interaction (EEI) is not effectively screened for electrons that are close to the surface. The fraction of these electrons and correspondingly an average EEI is larger in a wire with larger width-to-

thickness ratio. Superconductivity competes with EEI and is more easily suppressed in such wires. Qualitatively similar behavior was observed in wide MoGe stripes [26].

We do not find any evidence that the wire length or normal state resistance affect superconductivity. This is further confirmed by measurements on wires A, C, and J that have 4-probe electrode geometry shown in Fig. 1C. We found no difference in measurements done in quasi-4-probe (Fig. 1B) and 4-probe geometry, which implies that superconductivity in MoGe wires is not influenced by electrodes.

The Anderson localization theory predicts that one-electron states in a disordered wire decay exponentially with a localization length, which can be estimated as $\xi_A = 2Ak_F^2\ell/3\pi^2$ [27]. Following Ref. [28], we used for a mean free path in MoGe a value $\ell=0.3$ nm and estimated the Fermi vector k_F from the equation $1/\rho = (\epsilon^2k_F^2\ell)/(3\pi^2\hbar)$, which gives $k_F=1.6 \text{ \AA}^{-1}$. We estimated that for wire F $\xi_A \approx 300$ nm, which is much smaller than the length of the wire (25 μm). Therefore, wire F can be identified as a *localized superconductor*. The term, introduced by Ma and Lee [29], describes a system in which superconducting pairing occurs between time-reversed localized one-electron states. Our observation suggests that the long-range behavior of one-electron wave functions is not important for setting superconductivity.

For thickest wires A,B and C, the $\rho_L(T)$ dependence can be well-explained by the theory of thermally-activated phase slips (TAPS), as shown in Fig. 2A (we followed the procedure given in Refs.[16] and [30]). Fitting parameters (T_c and the zero-temperature Ginzburg-Landau coherence length $\xi(0)$) are $T_c=3.4$ K, $\xi(0)=9$ nm for wire A and $T_c=3.2$ K, $\xi(0)=9$ nm for wire B. For thinner wires, fitting with the TAPS theory returns unreasonably high values of T_c and $\xi(0)$. This trend, observed also in short MoGe [31] and Nb [32] nanowires, possibly reflects a proximity to a zero-temperature quantum phase transition, where $\xi(0)$ is expected to diverge. The deviation from the TAPS behavior could be due to an additional contribution from quantum phase slips. However, for all superconducting wires we observe a single-step transition without any characteristic features of QPS process such as a ‘‘tail’’ or positive curvature in $\rho_L(T)$ curves, or saturation to a constant resistivity at low temperatures. Our data are markedly different from the results on series of MoGe nanowires reported by Lau *et al.*[16], where the QPS contribution was used to explain behavior of $\rho_L(T)$ dependence.

We can also compare our results with the large set of data on short $\text{Mo}_{78}\text{Ge}_{22}$ nanowires fabricated by the molecular template technique with length in the range 30-300 nm reported by Bollinger *et al.* [15]. All wires in this set do not show the QPS or crossover behavior; instead a direct SIT was observed with a separatrix set

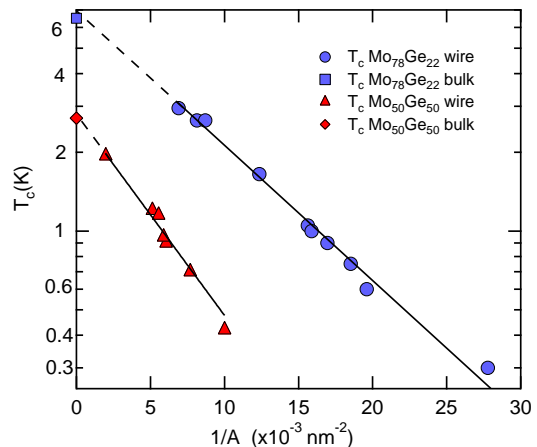


FIG. 3: Critical temperature of $\text{Mo}_{78}\text{Ge}_{22}$ and $\text{Mo}_{50}\text{Ge}_{50}$ nanowires as a function of the inverse of the wire cross sectional area. Solid lines represent an exponential form. The dashed lines indicate the extension of the exponential dependence to $1/A = 0$. Squares indicate the critical temperature of corresponding bulk alloys.

by total wire resistance equal to $R_Q = 6.45$ k Ω . The main evidence for this observation comes from wires with length smaller than 100 nm. At low temperatures superconductivity in these wires can be affected by the proximity effect because of the attached superconducting electrodes. We found that, if nanowires with length smaller than 100 nm are excluded, the data provided by Bollinger match well the data for our long nanowires when plotted in the $\rho_L(T)$ form. Both sets show a progressive shift of T_c with decreasing cross sectional area and approximately the same critical value of $\rho_L \approx 40$ Ω/nm separating insulating and superconducting regimes.

For each wire we define an empirical mean-field critical temperature, T_c , at the middle of the transition. T_c is plotted in Fig. 3 as a function of $1/A$ for two series of wires fabricated from $\text{Mo}_{78}\text{Ge}_{22}$ and $\text{Mo}_{50}\text{Ge}_{50}$ alloys. For $\text{Mo}_{50}\text{Ge}_{50}$, A was computed from $A = \rho L/R_{RT}$, with $\rho=235$ $\mu\Omega\text{cm}$ determined in separate measurements on film samples. Remarkably, the data for both series can be fitted by an exponential dependence $T_c = T_{c0}\exp(-\beta/A)$, shown as a solid line in the figure. The fitting parameter T_{c0} agrees with the indicated bulk critical temperature of the corresponding alloy. The second fitting parameter is $\beta = 120$ nm^2 for $\text{Mo}_{78}\text{Ge}_{22}$ and $\beta = 180$ nm^2 for $\text{Mo}_{50}\text{Ge}_{50}$.

Suppression of T_c by Coulomb repulsion was analyzed theoretically for the crossover region from 2D to 1D [2, 33], and the theory was compared with the behavior of T_c in Pb stripes [34]. However, we found that there is a quantitative disagreement between the theory and our data. For example, we observe that for a $\text{Mo}_{78}\text{Ge}_{22}$ wire A with an estimated thickness 6 nm and sheet resistance

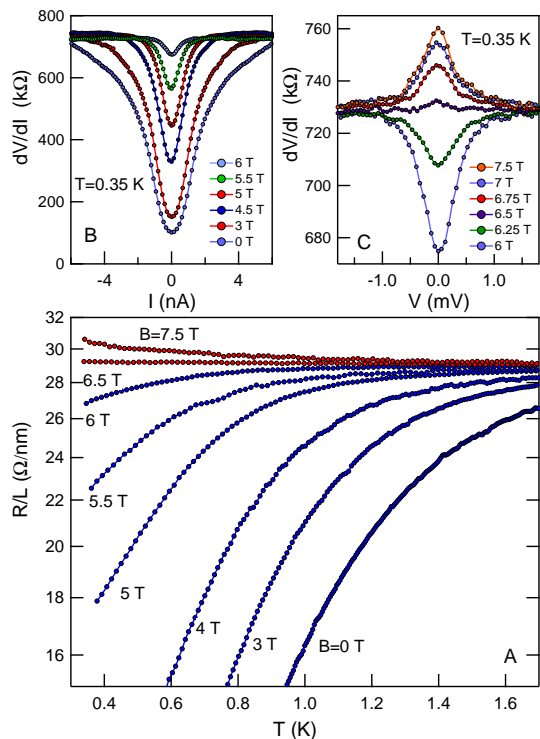


FIG. 4: (A) Temperature dependence of resistance per unit length for a nanowire F1 at indicated magnetic fields. (B) Differential resistance as function of current at $T=0.35$ K in superconducting regime at indicated magnetic fields. (C) Differential resistance as a function of bias voltage at $T=0.35$ K in the transitional regime of the SIT.

$R_{\square} \approx 230 \Omega$, reduction of the width from infinity (2D limit) to 25 nm reduces the critical temperature from 5.5 to 3 K. On the other hand, when we followed numerical routines given in Ref.[2] we found that essentially no T_c reduction is expected. The discrepancy can also be noticed directly from a comparison with the experimental data on the Pb stripe with width 22 nm that, unlike the MoGe wire, show no detectable T_c reduction compared to the 2D case [34]. The fermionic theories we used for the analysis do not include the effect of the Coulomb interaction on the single-particle density of states. Adding this contribution, as it was done for MoGe films [35], may perhaps improve an agreement with the experiment.

In Fig.4A we plot $\rho_L(T)$ of wire F1 at different magnetic fields (applied normal to the wire and substrate). Comparison of the data shown in Figs. 2 and 4 indicates that the evolution of the resistance in the critical regime is qualitatively the same for transitions driven by the magnetic field or reduction of A . In both cases, the transition from superconducting to insulating behavior in $\rho_L(T)$ curves is accompanied by the sign change of the zero-bias anomaly (ZBA) in differential resistance as shown in Fig. 4C. It is likely that in both cases the same

physics controls the critical regime of the SIT. For superconducting wires far from the critical field (shown as a function of current in Fig. 4B) simply reflects the decrease of the critical current of a wire. The origin of the ZBA in insulating and transitional regimes is not well understood.

1D superconductors do not allow formation of vortices; instead magnetic field penetrates a wire and uniformly suppresses the amplitude of the order parameter. The suppression of superconductivity by a magnetic field in 1D is a local fermionic process. Using parameters of nanowire F1 (mean-field $T_c = 0.9$ K, estimated width $w = 10$ nm, $D = 0.5$ cm/s² [26], spin-orbit scattering time $\tau_{so} \approx 5 \times 10^{-14}$ s [30]) we estimated suppression of T_c from standard formulas for the orbital ($\alpha_o = Dw^2e^2B^2/6\hbar$) and spin ($\alpha_s = \hbar\tau_{so}e^2B^2/2m^2$) pair-breakers [4]. Since both contributions are quadratic in magnetic field we used the formula $1.76k_B T_c = 2\alpha = 2(\alpha_o(B_c) + \alpha_s(B_c))$ and found that $B_c \approx 6$ T. It agrees with the experimental value $B_c \approx 6.5$ T. The agreement suggests that the zero-field T_c even for our thinnest wires should be interpreted as a usual mean-field critical temperature reflecting the reduced magnitude of the order-parameter.

In summary, we observed the superconductor-insulator transition in a series of long MoGe nanowires. The SIT, which likely has fermionic nature, can be driven by wire cross section and by magnetic field. Our results are not consistent with any of the currently known theories of the SIT in particular with the theory of quantum phase slips [3] and the Chakravarty-Schmid-Bulgadaev theory of dissipative phase transition [36], which was used to explain the SIT in short nanowires.

The authors thank A.M. Finkel'stein, L.B. Ioffe, E.G. Mishchenko, D. Mozyrsky, Y. Oreg, and M.E. Raikh for valuable discussions and B. Baker, M.C. DeLong, and R.C. Polson for technical support. Sample fabrication was carried out at the University of Utah Microfab and USTAR facilities. This work is supported by NSF CAREER Grant DMR 0955484.

-
- [1] T. Giamarchi, *Quantum Physics in One Dimension*, Oxford: New York (2004).
 - [2] Y. Oreg and A.M. Finkelstein, Phys. Rev. Lett. **83**, 191 (1999).
 - [3] K.Y. Arutyunov, D.S. Golubev, and A.D. Zaikin, Phys. Rep. **464**, 1-70 (2008).
 - [4] M. Tinkham, *Introduction to Superconductivity*, 2nd ed.; McGraw-Hill: New York (1996).
 - [5] D. Meidan, Y. Oreg, and G. Refael, Phys. Rev. Lett. **98**, 187001 (2007).
 - [6] A.D. Zaikin, D.S. Golubev, A. van Otterlo, and G.T. Zimanyi, Phys. Rev. Lett. **78**, 1552 (1997).

- [7] S. Sachdev, P. Werner, and M. Troyer, Phys. Rev. Lett. **92**, 237003 (2004).
- [8] S. Khlebnikov, Phys. Rev. B **77**, 014505 (2008).
- [9] H.P. Buchler, V.B. Geshkenbein, and G. Blatter, Phys. Rev. Lett. **92**, 067007 (2004).
- [10] J.A. Hoyos, C. Kotabage, and T. Vojta, Phys. Rev. Lett. **99**, 230601 (2007).
- [11] H.C. Fu, A. Seidel, J. Clarke, and D.-H. Lee, Phys. Rev. Lett. **96**, 157005 (2006).
- [12] M. Tian, N. Kumar, S. Xu, J. Wang, J.S. Kurtz, and M.H.W. Chan, Phys. Rev. Lett. **95**, 076802 (2005).
- [13] M. Singh, J. Wang, M. Tian, T.E. Mallouk, and M.H.W. Chan, Phys. Rev. B **83**, 220506 (2011).
- [14] A. Bezryadin, C.N. Lau, and M. Tinkham, Nature **404**, 971 (2000).
- [15] A.T. Bollinger, R.C. Dinsmore, A. Rogachev, and A. Bezryadin, Phys. Rev. Lett. **101**, 227003 (2008).
- [16] C.N. Lau, N. Markovic, M. Bockrath, A. Bezryadin, and M. Tinkham, Phys. Rev. Lett. **87**, 217003 (2001).
- [17] N. Giordano and E.R. Schuler, Phys. Rev. Lett. **63**, 2417 (1989).
- [18] K. Xu and J.R. Heath, Nano Lett. **8**, 136 (2008).
- [19] F. Altomare, A.M. Chang, M.R. Melloch, Y. Hong, and C.W. Tu, Phys. Rev. Lett. **97**, 017001 (2006).
- [20] M. Zgrinski, K.-P. Riikonen, V. Touboltsev, and K. Arutyunov, Nano Lett. **5**, 1029-1033 (2005).
- [21] A. Bezryadin and P.M. Goldbart, Adv. Mater. **22**, 1111-1121 (2010).
- [22] H. Namatsu *et al.*, J. Vac. Sci. Technol. B, **16**, 69 (1998).
- [23] J.K.W. Yang *et al.* J. Vac. Sci. Technol. B **27** 2622 (2009).
- [24] Supplementary materials.
- [25] B.L. Altshuler and A.G. Aronov, in *Electron-Electron Interaction in Disordered Systems*, eds. A.L. Efros and M. Pollak, Elsevier Science Publ. (1985).
- [26] J.M. Graybeal, P.M. Mankiewich, R.C. Dynes, and M.R. Beasley, Phys. Rev. Lett. **59**, 2697 (1987).
- [27] D.J. Thouless, Phys. Rev. Lett. **39**, 1167 (1977).
- [28] J.M. Graybeal, PhD thesis, Stanford University (1985).
- [29] M. Ma and P.A. Lee, Phys. Rev. B **32**, 5658 (1985).
- [30] A. Rogachev, A.T. Bollinger, and A. Bezryadin, Phys. Rev. Lett. **94**, 017004 (2005).
- [31] A. Rogachev, T.-C. Wei, D. Pekker, A.T. Bollinger, P.M. Goldbart, and A. Bezryadin, Phys. Rev. Lett. **97**, 137001 (2006).
- [32] A. Rogachev and A. Bezryadin, Appl Phys. Lett. **83**, 512-514 (2003).
- [33] R.A. Smith, B.S. Handy, and V. Ambegaokar, Phys. Rev. B **63**, 094513 (2001).
- [34] F. Sharifi, A.V. Herzog, and R.C. Dynes, Phys. Rev. Lett. **71**, 428 (1993).
- [35] T.R. Kirkpatrick and D. Belitz, Phys. Rev. Lett. **68**, 3232 (1992).
- [36] S. Chakravarty, Phys. Rev. Lett. **49**, 681 (1982); A. Schmid, *ibid.* **51**, 1506 (1983); S. A. Bulgadaev, JETP Lett. **39**, 315 (1984).